scientific reports

Check for updates

OPEN

5G NR sub-THz fiber-wireless integrated systems using polarization multiplexing-multiband technique and self-polarization diversity scheme

Ming-Chung Cheng[1], Hai-Han Lu[1]✉, Hsiao-Mei Lin[2], Stotaw Talbachew Hayle[1], Xu-Hong Huang[3], Wei-Wen Hsu[1], Yu-Chen Chung[1], Yu-Yao Bai[1], Kelper Okram[1] & Jia-Ming Lu[1]

Fifth generation (5G) new radio (NR) fiber-wireless integrated systems using polarization multiplexing-multiband technique and self-polarization diversity scheme are successfully implemented. Polarization multiplexing-multiband technique is an effectual method to enhance the transmission capacity and spectral efficiency of systems. Self-polarization diversity scheme is an efficient scheme for polarization demultiplexing, in which an *x*-polarized (*y*-polarized) optical carrier with multiple *x*-polarized (*y*-polarized) optical signals can be detected using single-ended photodiodes. The transmission of 5G NR sub-terahertz (THz) signals through fiber-wireless integrated systems holds promise to afford high-speed and long-haul wired-wireless communications. It shows the robustness to achieve high aggregate data rates and lays the foundation to meet the evolving demands of future communication systems. Through an integrated medium of 20 km single-mode fiber, 1.6 km optical wireless, and 4/8/12 m 5G NR wireless, four 5G sub-THz 32-quadrature amplitude modulation-orthogonal frequency-division multiplexing signals at *x*- and *y*-polarizations are transmitted with good transmission performance in terms of low bit error rates and error vector magnitudes. The successful transmission of sub-THz signals at different carrier frequencies and polarizations over fiber-wireless integrated systems proves system's ability to support cutting-edge 5G NR fiber-wireless integrated systems.

The arrival of the fifth-generation (5G) era has triggered a surge in innovative applications such as autonomous vehicles, 5G drones, mixed reality, 5G Internet of Everything, and ultra-high-speed video streaming[1–7]. However, these new applications impose higher requirements in terms of high data rate, stable connection stability, and low latency. To meet these increasing requirements, researchers have turned their attention to the development of sub-terahertz (sub-THz) communications. This cutting-edge technology enables the extension of 5G new radio (NR) into higher frequency bands, specifically the sub-THz frequencies spectrum spanning 100 to 300 GHz. The sub-THz band has huge potential to meet the data transmission requirements of various emerging 5G applications. Its inherent high-frequency characteristics make it particularly suitable for short-distance fast data transmission scenarios. Therefore, communication systems utilizing 5G NR in the sub-THz frequencies are attracting attention owing to their ability to provide fast data transmission over short distances[8–12]. The high-frequency band used in 5G NR sub-THz communications is susceptible to atmospheric absorption and attenuation, resulting in limited transmission range, especially in sparsely populated regions. In sparsely populated regions, 5G NR sub-THz communications are not the first choice to provide wide coverage and high penetration through obstacles. Integrating optical wireless communication (OWC) with short-distance 5G NR sub-THz communication can address the limitations of the latter, particularly in terms of range coverage. OWC utilizes modulated laser light to transport optical signals through free space, offering high-speed and long-distance communications[13–16]. When combined with 5G NR sub-THz communication, OWC can extend

[1]Institute of Electro-Optical Engineering, National Taipei University of Technology, Taipei 10608, Taiwan. [2]Department of Interaction Design, National Taipei University of Technology, Taipei 10608, Taiwan. [3]The School of Information Science and Engineering, Fujian University of Technology, Fujian 350118, China. ✉email: hhlu@ntut.edu.tw

the reach of 5G NR connectivity, effectively enhancing both speed and distance capabilities. Transporting 5G NR sub-THz signals through fiber-wireless integrated systems, as depicted in Fig. 1, holds promise for providing high-speed and long-haul wired-wireless transmissions. It takes advantage of optical fiber communications to achieve large capacity and long-haul transmission, and the advantages of OWC to expand coverage beyond the limitations of 5G wireless communications. Consequently, the 5G NR sub-THz fiber-wireless integrated system emerges as an advanced communication infrastructure that can meet the growing demand for high-speed and long-haul communications in modern networks.

In the following, we report and implement a 5G NR sub-THz fiber-wireless integrated system using polarization multiplexing-multiband technique and self-polarization diversity scheme. Polarization multiplexing-multiband technique is an effectual way to enhance the transmission capacity and spectral efficiency of fiber-wireless integrated systems.In addition, to further increase the transmission capacity and spectral efficiency, quadrature amplitude modulation (QAM)-orthogonal frequency-division multiplexing (OFDM) modulation is adopted. QAM-OFDM modulation is a robust modulation that meets the requirements of high transmission capacity and improved spectral efficiency. However, combining the polarization multiplexing-multiband technique with QAM-OFDM modulation poses challenges, primarily requiring sophisticated polarization tracking scheme, complex digital signal processing approach, and costly balanced photodiode (PD) for polarization demultiplexing[17–19]. They will restrict the feasibility of 5G NR sub-THz fiber-wireless integrated systems utilizing polarization multiplexing-multiband technique. To address these challenges, a self-polarization diversity scheme is thus employed. The self-polarization diversity scheme is an effective scheme for polarization demultiplexing, in which an x-polarized (y-polarized) optical carrier with multiple x-polarized (y-polarized) optical signals can be detected using single-ended PDs[20,21]. It is attractive since it doesn't require complex polarization tracking scheme, complicated digital signal processing approach, and costly balanced PD[22].

This demonstration highlights the possibility of utilizing sub-THz frequencies for 5G NR communications in fiber-wireless integrated systems by employing polarization multiplexing-multiband technique and self-polarization diversity scheme. It shows the capability to achieve high aggregate data rates and lays the foundation for further developments in next-generation communication systems. The 5G NR sub-THz fiber-wireless integrated system comprises multiple transmission media, including 20 km single-mode fiber (SMF), 1.6 km optical wireless link, and 5G NR wireless transmission at various distances (4 m, 8 m and 12 m). System utilizes four sub-THz frequencies and two orthogonal polarizations. Each frequency at *x*- and *y*-polarizations carries a 25-Gbps signal using 32-QAM-OFDM. By transporting hybrid sub-THz signals, system achieves an impressive total data rate of 200 Gbps (25 Gbps/carrier frequency/polarization × 4 carrier frequencies × 2 polarizations). The link performance of various 5G NR sub-THz signals is evaluated at frequencies of 180, 210, 240, and 270 GHz and at both *x*- and *y*-polarizations. Performance metrics such as bit error rates (BERs) and error vector magnitudes (EVMs) are used to assess system's performance. Over a cross medium of 20 km SMF, 1.6 km optical wireless, and 4/8/12 m 5G NR wireless, four 5G sub-THz 32-QAM-OFDM signals at *x*- and *y*-polarizations are transmitted with good transmission performance, evidenced by low BERs ($< 3.8 \times 10^{-3}$ forward error correction (FEC) limit) and EVMs ($< 10\%$)[22]. Previous research presented the achievability of an integrated fiber-free-space optical (FSO)-5G NR sub-THz link with a total data rate of 86.112 Gbps[23]. However, the total data rate of 86.112 Gbps is much smaller than the associated value of 200 Gbps achieved in this proposed 5G NR sub-THz fiber-

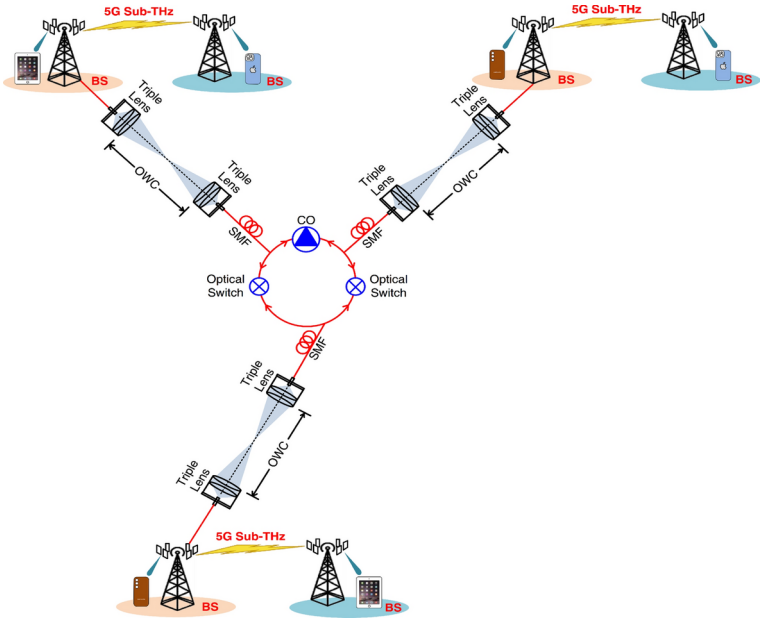

Fig. 1. Transporting 5G NR sub-THz signals over fiber-wireless integrated systems. Transporting 5G NR sub-THz signals through fiber-wireless integrated systems holds promise for providing high-speed and long-haul wired-wireless transmissions.

wireless integrated system. Moreover, the 500 m FSO link is much shorter than the associated value of 1.6 km transmitting in this integrated system. In addition, a single channel 16-QAM-OFDM signal transmission at 408 GHz over a 10.7-m wireless link was successfully built[24]. Nevertheless, this research concentrated on THz wireless links, it had not integrated fiber-optical wireless links. In actual links, THz wireless links must combine with fiber-optical wireless links to expand the coverage of THz communications. The practicability of a combined fibre/FSO communication system at millimeter-wave/sub-THz frequencies was practically demonstrated[25]. Nonetheless, it requires complex single optical carrier modulation technique. Furthermore, the aggregate data rate of 56.34 Gbps is much lower than the related value of 200 Gbps implemented in this demonstrated system. Moreover, the 1.2 km FSO link is shorter than the relevant value of 1.6 km transmitting in this demonstration. In this demonstration, the achieved low BERs and EVMs disclose that this demonstrated fiber-wireless integrated system, which incorporates polarization multiplexing-multiband technique and self-polarization diversity scheme, shows promise for 5G NR communications in the sub-THz frequencies. The successful transmission of sub-THz signals at different carrier frequencies and polarizations over fiber-wireless integration proves system's ability to implement a cutting-edge 5G NR fiber-wireless integrated system.

Results and discussion

Optical spectrum of one unmodulated *x*-polarized/*y*-polarized optical carrier and eight orthogonal polarized optical signals (four *x*-polarized and four *y*-polarized optical signals)

Figure 2(a) exhibits the optical spectrum of an unmodulated *x*-polarized optical carrier and eight orthogonal polarized optical signals (four *x*-polarized and four *y*-polarized optical signals) modulated with 25 Gbps 32-QAM-OFDM signal. Clearly, eight orthogonal polarized optical signals (four *x*-polarized and four *y*-polarized optical signals) are carried by an *x*-polarized optical carrier. With 110–220 GHz (220–320 GHz) uni-travelling carrier (UTC)-PD detection, 25-Gbps/180-GHz and 25-Gbps/210-GHz (25-Gbps/240-GHz and 25-Gbps/270-GHz) sub-THz signals are generated from the beating effect between the unmodulated *x*-polarized optical carrier and the other two *x*-polarized optical signals that are spaced at 180 and 210 GHz (240 and 270 GHz) frequencies. In addition, after the *x*-polarized optical carrier is polarization-rotated from *x*-polarization to *y*-polarization, the optical spectrum of one unmodulated *y*-polarized optical carrier and eight orthogonal polarized optical signals (four *y*-polarized and four *x*-polarized optical signals) modulated with 25 Gbps 32-QAM-OFDM signal is presented in Fig. 2(b). Similarly, after detection by a 110–220 GHz (220–320 GHz) UTC-PD, 25-Gbps/180-GHz and 25-Gbps/210-GHz (25-Gbps/240-GHz and 25-Gbps/270-GHz) sub-THz signals are produced from the beating effect between the unmodulated *y*-polarized optical carrier and the other two *y*-polarized optical signals that are spaced at 180 and 210 GHz (240 and 270 GHz) frequencies.

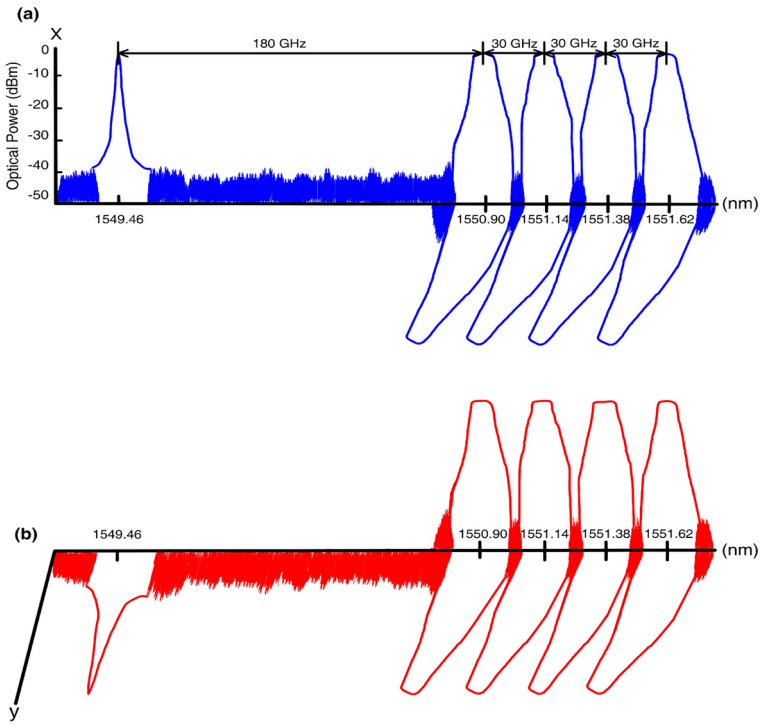

Fig. 2. Optical spectrum of one unmodulated *x*-polarized/*y*-polarized optical carrier and eight orthogonal polarized optical signals. **(a)** Optical spectrum of one unmodulated *x*-polarized optical carrier and eight orthogonal polarized optical signals (four *x*-polarized and four *y*-polarized optical signals) modulated with 25 Gbps 32-QAM-OFDM signal. **(b)** Optical spectrum of one unmodulated *y*-polarized optical carrier and eight orthogonal polarized optical signals (four *y*-polarized and four *x*-polarized optical signals) modulated with 25 Gbps 32-QAM-OFDM signal.

As an x-polarized optical carrier (OC_x) and eight orthogonal optical signals (OS_{x1}, OS_{x2}, OS_{x3}, OS_{x4}, OS_{y1}, OS_{y2}, OS_{y3}, and OS_{y4}) are detected by a single-ended PD, the related square law detection can be achieved as[26,27]:

$$\begin{aligned}&|OC_x + OS_{x1} + \cdots + OS_{x4} + OS_{y1} + \cdots + OS_{y4}|^2 \\ &= |OC_x|^2 + (|OS_{x1}|^2 + \cdots + |OS_{y4}|^2) + [2Re(OS_{x1}{\cdot}OS_{x2}) + \cdots + 2Re(OS_{y3}{\cdot}OS_{y4})] \\ &+ [2Re(OC_x{\cdot}OS_{x1}) + \cdots + 2Re(OC_x{\cdot}OS_{x4})] \\ &+ [2Re(OC_x{\cdot}OS_{y1}) + \cdots + 2Re(OS_{x4}{\cdot}OS_{y4})] \approx \\ &|OC_x|^2 + 2Re(OC_x{\cdot}OS_{x1}) + \cdots + 2Re(OC_x{\cdot}OS_{x4}),\end{aligned} \tag{1}$$

For the DC term ($|OC_x|^2$), it can be eliminated using a DC block. For the signal-to-signal beating interferences ($|OS_{x1}|^2 + \ldots + |OS_{y4}|^2 + 2\mathrm{Re}(OS_{x1}{\cdot}OS_{x2}) + \ldots + 2\mathrm{Re}(OS_{y3}{\cdot}OS_{y4})$), since there is a 180-GHz guard band between the unmodulated *x*-polarized optical carrier and the modulated *x*-polarized (*y*-polarized) optical signals, they will not degrade the system performance. As for the cross-beating interferences ($2\mathrm{Re}(OC_x{\cdot}OS_{y1}) + \ldots + 2\mathrm{Re}(OS_{x4}{\cdot}OS_{y4})$), the cross-beating interferences will be zero owing to the orthogonality of *x*-polarization and *y*-polarization. Through guard band protection and zero value of cross-beating interferences, the unmodulated *x*-polarized optical carrier with modulated *x*-polarized optical signals ($2\mathrm{Re}(OC_x{\cdot}OS_{x1}) + \ldots + 2\mathrm{Re}(OC_x{\cdot}OS_{x4})$) can be detected using single-ended PDs. In the same manner, the unmodulated *y*-polarized optical carrier with modulated *y*-polarized optical signals ($2\mathrm{Re}(OC_y{\cdot}OS_{y1}) + \ldots + 2\mathrm{Re}(OC_y{\cdot}OS_{y4})$) can be detected using single-ended PDs.

Evaluation of BERs of 25-Gbps 32-QAM-OFDM signal for various transmission scenarios at different carrier frequencies and polarizations

Figures 3(a), (b), (c), and (d) exhibit the measured BERs against uni-travelling carrier (UTC)-PD-1 and UTC-PD-2 input powers, using 25-Gbps 32-QAM-OFDM signal at different carrier frequencies of 180, 210, 240, and 270 GHz and different polarizations of *x*- and *y*-polarizations. Under different transmission scenarios, including 20 km SMF, 1.6 km optical wireless, and several distances of sub-THz wireless transmissions, at suitable UTC-PD-1 and UTC-PD-2 input powers, the measured BER values are below the 3.8×10^{-3} FEC limit with 7% overhead (FEC 7%) at different carrier frequencies and polarizations. In the cases of 25-Gbps/180-GHz (x-polarization) [Fig. 3(a)] and 25-Gbps/210-GHz (y-polarization) [Fig. 3(b)] 32-QAM-OFDM signals transmission, lowest BERs of 3.7×10^{-4} and 4.5×10^{-4} (4 m wireless link), 8.6×10^{-4} and 1.1×10^{-3} (8 m wireless link), 2.1×10^{-3} and 3.2×10^{-3} (12 m wireless link) are obtained at optimum UTC-PD-1 input powers for different wireless link distances. It's noted that increasing UTC-PD-1 input powers initially decreases BER values until they reach the lowest values at different sub-THz wireless links. However, surpassing the optimum UTC-PD-1 input powers brings on the saturation of the sub-THz signal output powers. As the sub-THz signal output powers saturate, further increasing the UTC-PD-1 input powers doesn't decrease BER values but rather leads to their

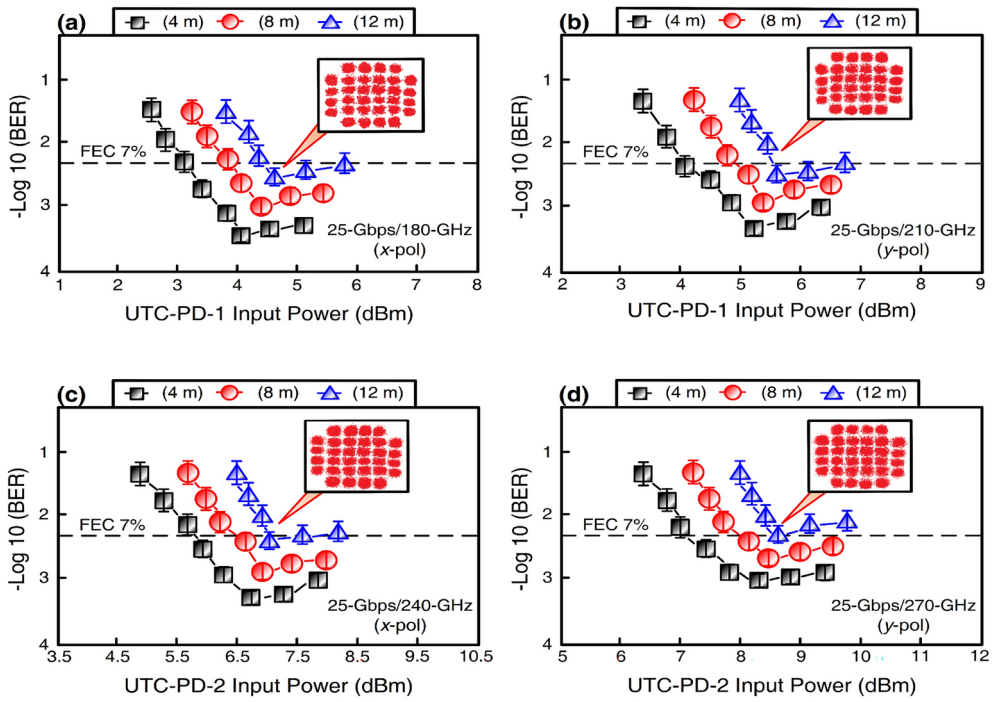

Fig. 3. Evaluation of BERs of 25-Gbps 32-QAM-OFDM signal for various transmission scenarios at different carrier frequencies and polarizations. Measured BERs against UTC-PD-1 and UTC-PD-2 input powers, using 25-Gbps 32-QAM-OFDM signal at different carrier frequencies and polarizations of **(a)** 180 GHz (*x*-polarization), **(b)** 210 GHz (*y*-polarization), **(c)** 240 GHz (*x*-polarization), and **(d)** 270 GHz (*y*-polarization).

increase[28,29]. Therefore, determining and maintaining optimum UTC-PD-1 input powers is crucial for achieving the lowest BER values. In addition, for 25-Gbps/240-GHz GHz (x-polarization) [Fig. 3(c)] and 25-Gbps/270-GHz GHz (y-polarization) [Fig. 3(d)] 32-QAM-OFDM signals transmission, lowest BER values of 6.3×10^{-4} and 8.4×10^{-4} (4 m wireless link), 1.3×10^{-3} and 2.5×10^{-3} (8 m wireless link), 3.5×10^{-3} and 3.8×10^{-3} (12 m wireless link) are attained at various wireless link distances. Similar to the behavior observed with UTC-PD-1 input powers, BERs decrease as UTC-PD-2 input powers increase until they reach their lowest values at specific input powers. Increasing the input powers to UTC-PD-2 beyond the optimal levels will bring on the saturation of sub-THz signal output powers. Since the sub-THz signal output powers are already saturated, increasing the UTC-PD-2 input powers will not cause a proportional decreasing in BERs. Furthermore, distinct constellations are observed for different carrier frequencies and polarizations. These distinct constellations, combined with BER values below the FEC 7% threshold, demonstrate the feasibility of sub-THz signal transmission at different carrier frequencies and polarizations over fiber-wireless integrated systems.

Analysis of EVMs of 25-Gbps 32-QAM-OFDM signals for various transmission scenarios at different carrier frequencies and polarizations

Figure 4 present the measured EVMs versus UTC-PD-1 and UTC-PD-2 input powers over three different media of 20 km SMF, 1.6 km optical wireless, and 12 m sub-THz wireless, using 25-Gbps 32-QAM-OFDM signal at different carrier frequencies of 180, 210, 240, and 270 GHz and different polarizations. Similar to the operation in BERs, for 25-Gbps/180-GHz and 25-Gbps/240-GHz signals, *x*-polarization is chosen; for 25-Gbps/210-GHz and 25-Gbps/270-GHz signals, *y*-polarization is chosen. The measured EVMs are required to be below the 10% requirement for suitable UTC-PD-1 and UTC-PD-2 input powers at various carrier frequencies and polarizations. For 25-Gbps/180-GHz (*x*-polarization) 32-QAM-OFDM signal transmission, an 8.4% minimum EVM is attained at 6.2 dBm UTC-PD-1 input power. In addition, for 25-Gbps/210-GHz (*y*-polarization), 25-Gbps/240-GHz (*x*-polarization), and 25-Gbps/270-GHz (*y*-polarization) 32-QAM-OFDM signals transmission, 9%, 9.5%, and 10%minimum EVMs, respectively, are attained at 6.7, 7.2, and 7.8 dBm UTC-PD-1 and UTC-PD-2 input powers. Increasing UTC-PD-1/UTC-PD-2 input powers initially decreases EVMs until they reach their lowest values. Beyond the specific input powers, the sub-THz signal output powers saturate, causing an increase in EVMs. Thus, determining the specific UTC-PD-1/UTC-PD-2 input powers for achieving the desired EVMs in the transmission of 25-Gbps 32-QAM-OFDM signals at various carrier frequencies and polarizations is vitally important. If UTC-PD-1/UTC-PD-2 input powers increase beyond the specific values, the EVMs start to increase. To attain the lowest EVMs in a 5G NR sub-THz fiber-wireless integrated system, it is important to find the trade-off points where increasing UTC-PD-1/UTC-PD-2 input powers results in an increase in EVMs rather than a decrease. In addition, increasing the carrier frequency from 180 to 270 GHz at both polarizations requires higher UTC-PD-1/UTC-PD-2 input powers to maintain acceptable EVMs. This requirement is required due to the reduced signal-to-noise ratio at higher carrier frequencies. Higher carrier frequencies introduce higher white noise and phase noise, which degrades transmission performance and thereby require higher input power to maintain transmission quality[30,31].

Methods

5G NR sub-THz *fiber*-wireless integrated system using polarization multiplexing-multiband technique and self-polarization diversity scheme

Figure 5 exhibits the structure of the 5G NR sub-THz fiber-wireless integrated system using polarization multiplexing-multiband technique and self-polarization diversity scheme, at different carrier frequencies of 180, 210, 240, and 270 GHz and different polarizations of *x*- and *y*-polarizations. A picture of experimental setup is presented in Fig. 6. Transmission is achieved through 20 km SMF, 1.6 km optical wireless, and several distances of sub-THz wireless link. Firstly, an optical comb source produces 10 optical carriers with 30 GHz spacing, ranging from 1549.46 nm to 1551.62 nm. The output from the optical comb source is split using a 1×2 optical

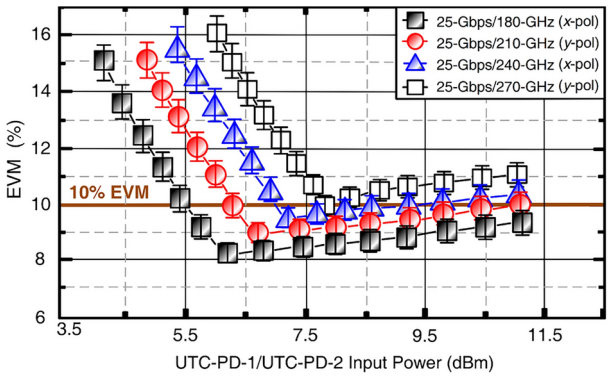

Fig. 4. Analysis of EVMs of 25-Gbps 32-QAM-OFDM signals for various transmission scenarios at different carrier frequencies and polarizations. Measured EVMs versus UTC-PD-1 and UTC-PD-2 input powers over three different media of 20 km SMF, 1.6 km optical wireless, and 12 m sub-THz wireless, using 25-Gbps 32-QAM-OFDM signal at different carrier frequencies and polarizations.

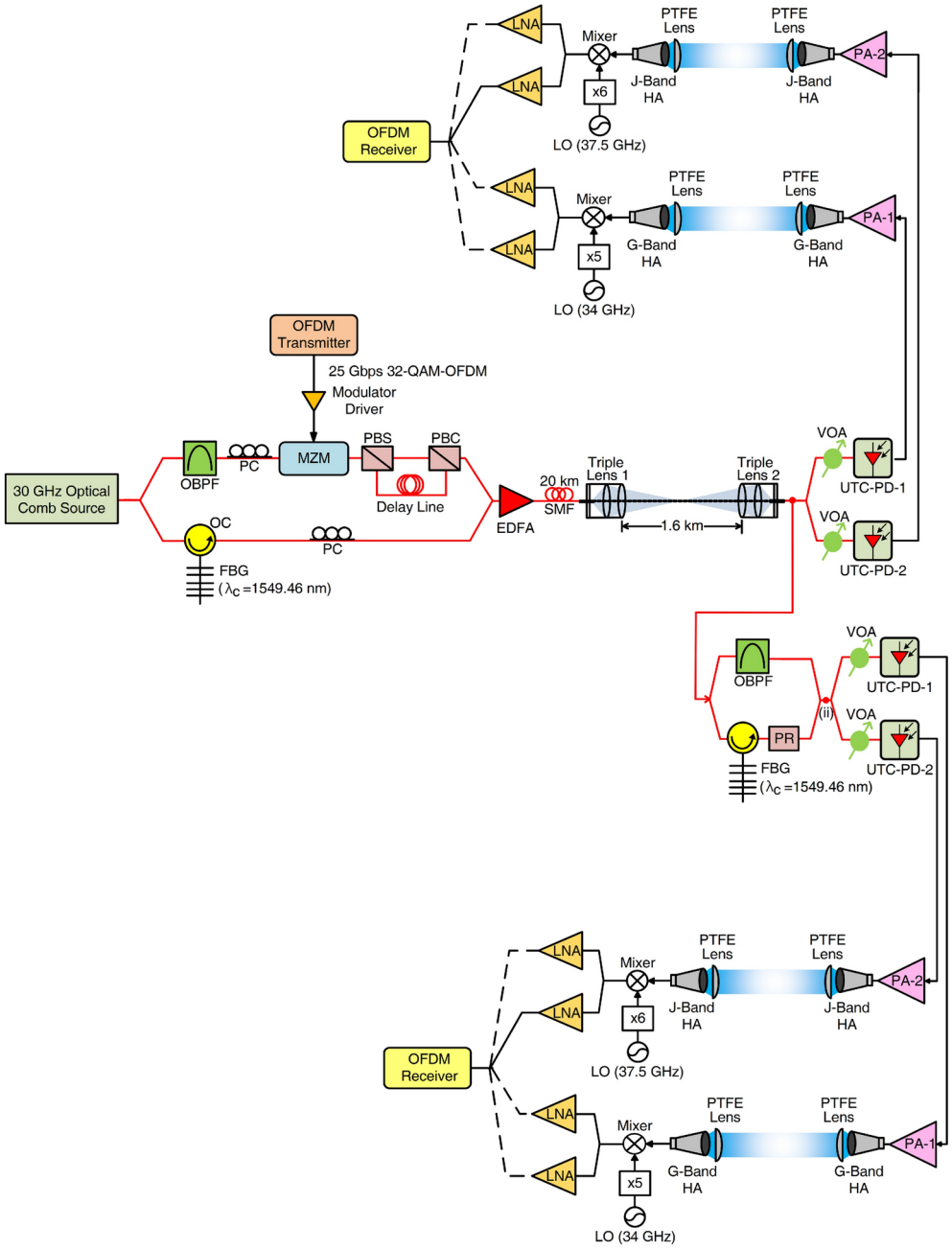

Fig. 5. 5G NR sub-THz fiber-wireless integrated system using polarization multiplexing-multiband technique and self-polarization diversity scheme. Structure of the 5G NR sub-THz fiber-wireless integrated system using polarization multiplexing-multiband technique and self-polarization diversity scheme, at different carrier frequencies of 180, 210, 240, and 270 GHz and different polarizations of *x*- and *y*-polarizations.

splitter, and went through an optical band-pass filter (OBPF) (upper path) and an optical circulator (OC) with a fiber Bragg grating (FBG) (lower path). The OBPF has a bandwidth of 2.4 nm and a filter slope of 850 dB/nm, and the FBG has a reflectivity of 99.7% at 1549.46 nm. For the upper path, four optical carriers selected by the OBPF are provided to a Mach–Zehnder modulator. A 25-Gbps 32-QAM-OFDM signal generated from an OFDM transmitter passes through a modulator driver, which then modulates the Mach–Zehnder modulator. Thus, each of the four optical carriers is driven by a 25-Gbps 32-QAM-OFDM signal. A polarizing beam splitter splits the four modulated optical signals into two orthogonal polarizations (*x*- and *y*-polarizations). An optical delay line is used to make up for phase mismatch. The four *x*- and *y*-polarized modulated optical signals are recombined through a polarization beam combiner. For the lower path, one optical carrier picked up by the OC with an FBG serves as an optical local oscillator (LO). Four modulated optical signals of *x*- and *y*-polarizations are spaced from the optical LO at 180, 210, 240, and 270 GHz. Next, one unmodulated *x*-polarized optical carrier and eight orthogonal polarized modulated optical signals are integrated by a 2×1 optical coupler,

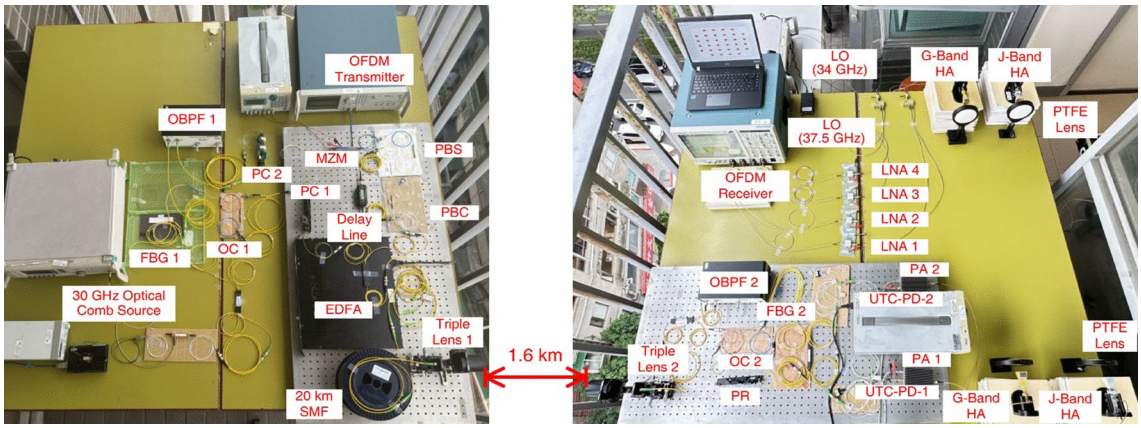

Fig. 6. A picture of experimental setup.

intensified by an erbium-doped fiber amplifier (EDFA), and transported through 20 km SMF with 1.6 km free space using a pair of triplet lenses. A pair of triplet lenses, comprising convex lens, concave lens and convex lens, are used to facilitate the long-distance optical wireless link[32]. The triplet lens at the receiver performs as a focus device to accurately focus laser beam on the fiber ferrule input despite the challenges posed by the 1.6 km optical wireless link. After 1.6 km optical wireless link, one unmodulated *x*-polarized optical carrier and eight orthogonal polarized modulated optical signals are separated into two parts. For the upper part, the unmodulated optical carrier and modulated optical signals are separated by an optical splitter, attenuated by two separate variable optical attenuators (VOAs), and detected by a UTC-PD-1 operating in 110–220 GHz frequency range and a UTC-PD-2 functioning in 220–320 GHz frequency range. With self-polarization diversity scheme, four *x*-polarized modulated optical signals are detected with an optical carrier in *x*-polarization by two single-ended UTC-PDs. With 180 GHz guard band protection, UTC-PD-1 produces 25-Gbps/180-GHz and 25-Gbps/210-GHz 32-QAM-OFDM electrical signals. These sub-THz electrical signals are enhanced by a power amplifier (PA-1) operating in 170–260 GHz frequencies. The enhanced signals are transmitted wirelessly via horn antennas (HAs) functioning in the 140–220 GHz G-band. Sub-THz wireless link uses a pair of PTFE (polytetrafluoroethylene) lenses working at sub-THz frequencies to enable further wireless transmission[33,34]. After wireless transmission at 4 m, 8 m, and 12 m, the sub-THz signals are down-converted by a mixer driven by a 5th-order frequency multiplier with a 34-GHz LO. After down-conversion, the central frequencies of down-converted signals are 10 GHz (180 – 34×5) and 40 GHz (210 – 34×5). The down-converted signals are then enhanced by two independent low noise amplifiers (LNAs) operating in 0.01 to 26.5 GHz and 33–50 GHz frequency range. The enhanced signals are subsequently provided to the OFDM receiver for performance evaluation. In addition, protection by the 180 GHz guard band, UTC-PD-2 generates 25-Gbps/240-GHz and 25-Gbps/270-GHz 32-QAM-OFDM electrical signals. These signals are then enhanced by a power amplifier (PA-2) that operates in the frequencies of 220–330 GHz. The enhanced signals are transported wirelessly via HAs operating in the 220–325 GHz J-band. The sub-THz wireless link utilizes a pair of PTFE lenses functioning at sub-THz frequencies to enable further wireless transmission. These sub-THz signals are down-converted to intermediate frequencies utilizing mixers over 4 m, 8 m and 12 m wireless links. A mixer, driven by a 6-order frequency multiplier with a 37.5-GHz LO, down-converts the signals. The center frequencies after down-conversion are 15 GHz (240 – 37.5×6) and 45 GHz (270 – 37.5×6). Subsequently, the down-converted signals are amplified using two independent LNAs functioning at 10 MHz-26.5 GHz and 33–50 GHz frequencies. The amplified signals are sent to the OFDM receiver for performance analysis.

For the lower part, one unmodulated *x*-polarized optical carrier and eight orthogonal polarized optical signals are divided utilizing an optical splitter. Eight orthogonal polarized optical signals are filtered utilizing an OBPF (upper path), and one unmodulated *x*-polarized optical carrier is picked up using an OC with an FBG and polarization-rotated using a polarization rotator (lower path). Recombining the *y*-polarized optical carrier with the eight orthogonal polarized optical signals, one unmodulated *y*-polarized optical carrier with four *y*-polarized and four *x*-polarized optical signals is attained. The combined optical carrier and optical signals are separated by a 1×2 optical splitter, controlled by separated VOAs, and detected by a UTC-PD-1 working at 110–220 GHz frequencies and a UTC-PD-2 functioning at 220–320 GHz frequencies. With self-polarization diversity scheme, the four modulated optical signals in *y*-polarization are detected with an optical carrier in *y*-polarization by two single-ended UTC-PDs. UTC-PD-1 detects 25-Gbps/180-GHz and 25-Gbps/210-GHz 32-QAM-OFDM electrical signals. The detected sub-THz electrical signals are boosted by a power amplifier (PA-1) operating in 170–260 GHz frequencies. The boosted signals are transported wirelessly by a pair of HAs functioning in the 140–220 GHz G-band. The sub-THz beam is radiated through free space by a pair of PTFE lenses operating at sub-THz frequencies. The sub-THz signals are down-converted to the intermediate frequencies using a mixer with a 34-GHz electrical LO and a frequency multiplier with a factor of 5 over 4 m, 8 m, and 12 m wireless transmission. After promotion by two independent LNAs, an OFDM receiver captures the enhanced signal for further processing. Additionally, UTC-PD-2 detects 25-Gbps/240-GHz and 25-Gbps/270-GHz 32-QAM-OFDM electrical signals. A power amplifier (PA-2) working at 220–320 GHz frequencies amplifies the detected

Key points within the setup	Output of MZM	Output of OC with FBG	Output of EDFA	Output of 20 km SMF	Output of 1.6 km optical wireless link
Optical power level (dBm)	−3.2	−2.8	17	12.8	11

Table 1. The optical power levels at kye points within in the setup.

signals. The amplified signals are transmitted wirelessly through HAs functioning in the 220–325 GHz J-band. The sub-THz beam is emitted through free space via a set of PTFE lenses functioning at sub-THz frequencies. At wireless transmission distances of 4 m, 8 m, and 12 m, sub-THz signals are down-converted into microwave signals with 15 and 45 GHz center frequencies. The down-converted microwave signals are amplified using two independent LNAs. The amplified signals are successively captured by an OFDM receiver for further processing.

For better understanding, a table (Table 1) outlines the optical power levels at key points withinin the setup, such as the output of MZM, the output of OC with FBG, the output of EDFA, the output of 20 km SMF, and the output of 1.6 km optical wireless link.

Data availability

The datasets used and/or analysed during the current study available from the corresponding author on reasonable request.

Received: 24 August 2024; Accepted: 28 October 2024
Published online: 02 November 2024

References

1. Salvador, L. R. & Rajnai, Z. 5G networks in Spain: status, applications and opportunities. *IEEE 22nd World Symposium on Applied Machine Intelligence and Informatics (SAMI)* 000139–000142 (2024).
2. Pradeep, P., Kottareddygari, J. S. & Paidimarry, C. S. Design of a dual-band monopole antenna for Internet of Things and sub-6 GHz 5G applications. *IEEE Wireless Antenna and Microwave Symposium (WAMS)* 1–4 (2024).
3. Rawat, B. S., Srivastava, A., Shrivastava, V., Singh, G. & Garg, N. A comprehensive analysis of applications in Internet of Things networks in 5G and 6G. *2nd International Conference on Computer, Communication and Control (IC4)* 1–6 (2024).
4. Sood, S. A technical analysis of hybrid combination of AI, 5G, and ML for various application. *IEEE International Conference on Computing, Power and Communication Technologies (IC2PCT)* 1065–1070 (2024).
5. Rolland, J. P. & Goodsell, J. Waveguide-based augmented reality displays: a highlight. *Light Sci. Appl.* **13**, Art. no. 22 (2024).
6. Dalir, Z., Seddighi, F., Esmaily, H., Tashnizi, M. A. & Tabriz, E. R. Effects of virtual reality on chest tube removal pain management in patients undergoing coronary artery bypass grafting: a randomized clinical trial. *Sci Rep.* **14**, Art. no. 2918 (2024).
7. Petrizzo, I., Mikellidou, K., Avraam, S., Avraamides, M. & Arrighi, R. Reshaping the peripersonal space in virtual reality. *Sci Rep.* **14**, Art. no. 2918 (2024).
8. Chukhno, N. et al. Models, methods, and solutions for Mmulticasting in 5G/6G mmWave and sub-THz systems. *IEEE Commun. Surv. Tut.* **26**, 119–159 (2024).
9. Lu, H. H. et al. Two-way 5G NR fiber-wireless systems using single-carrier optical modulation for downstream and phase modulation scheme for upstream. *IEEE/OSA J. Light. Technol.* **41**, 1749–1758 (2023).
10. Ding, J. et al. THz-over-fiber transmission with a net rate of 5.12 Tbps in an 80 channel WDM system. *Opt. Lett.* **47**, 3103–3106 (2022).
11. Lu, H. H. et al. Bi-directional fiber-FSO-5G MMW/5G new radio sub-THz convergence. *IEEE/OSA J. Light. Technol.* **39**, 7179–7190 (2021).
12. de S. Lopes, C. H. et al. Non-standalone 5G NR fiber-wireless system using FSO and fiber-optics fronthauls. *IEEE/OSA J. Light. Technol.* **39**, 406–417 (2021).
13. Chow, C. W. et al. Actively controllable beam steering optical wireless communication (OWC) using integrated optical phased array (OPA). *IEEE/OSA J. Light. Technol.* **41**, 1122–1128 (2023).
14. Lu, H. H., Li, C. Y., Huang, X. H., Lin, C. J., Lin, R. D., Lin, Y. S., Tang, Y. S. & Fan, W. C. A combined fiber/free-space-optical communication system for long-haul wireline/wireless transmission at millimetre-wave/sub-THz frequencies. *Commun. Eng.* **2**, Art. no. 18 (2023).
15. Lu, H. H., Huang, X. H., Li, C. Y., Xu, Y. Z., Jin, J. L., Chen, W. X., Lin, C. H. & Wu, T. M. Two-way free-space optics-based interface between fiber and 5G communication employing polarisation-orthogonal modulation. *Commun. Eng.* **2**, Art. no. 89 (2023).
16. Jia, Z., Yu, J., Ellinas, G. & Chang, G. K. Key enabling technologies for optical–wireless networks: optical millimeter-wave generation, wavelength reuse, and architecture. *IEEE/OSA J. Light. Technol.* **25**, 3452–3471 (2007).
17. Li, C. Y. et al. A hybrid Internet/CATV/5G fiber-FSO integrated system with a triple-wavelength polarization multiplexing scenario. *IEEE Access* **7**, 151023–151033 (2019).
18. Shen, S. et al. Polarization-tracking-free PDM supporting hybrid digital-analog transport for fixed-mobile systems. *IEEE Photon. Technol. Lett.* **31**, 54–57 (2019).
19. Liu, S. J., Yan, J. H., Tseng, C. Y. & Feng, K. M. Polarization-tracking-free PDM IF-over-fiber mobile fronthaul employing multiband DDO-OFDM. *Conference on Lasers and Electro-Optics (CLEO)* **SF2F.3** (2016).
20. Chen, Y. W. et al. Over 210 Gb/s PDM multiband DDO-OFDM LR-PON downstream with simple self-polarization diversity. *Opt. Express* **23**, 18525–18533 (2015).
21. Xie, C. PMD insensitive direct-detection optical OFDM systems using self-polarization diversity. *Opt. Fiber Commun. Conf. (OFC)* **OMM2** (2008).
22. Acar, E. How error vector magnitude (EVM) measurement improves your system-level performance. Tech. Art. 1–6, Analog Devices, Inc. (2021).
23. Lu, H. H., Li, C. Y., Tsai, W. S., Lin, R. D., Tang, Y. S., Chen, Y. X., Lin, Y. S. & Fan, W. C. An integrated fiber-FSO-5G NR sub-THz link with 86.112 Gbps high aggregate data rates. *IEEE/OSA J. Light. Technol.* **40**, 7790–7798 (2022).
24. Jia, S. et al. Integrated dual-laser photonic chip for high-purity carrier generation enabling ultrafast terahertz wireless communications. *Nat. Commun.* **13**, Art. no. 1388 (2022).
25. Lu, H. H., Li, C. Y., Huang, X. H., Lin, C. J., Lin, R. D., Lin, Y. S., Tang, Y. S. & Fan, W. C. A combined fibre/free-space-optical communication system for long-haul wireline/wireless transmission at millimetre-wave/sub-THz frequencies. *Commun. Eng.* **2**, Art. no. 18 (2023).

26. Chen, Y. W., Tseng, C. Y., Liu, S. J. & Feng, K. M. PDM DDO-OFDM with self-polarisation diversity for the backhaul of radio-over-fiber system. *Opt. Fiber Commun. Conf. (OFC)* **Th4A.2** (2016).
27. Yan, K., Zhou, X., Liu, W. & Huo, J. PDM-DD-SSB-OFDM system based on a single-end PD for short reach communications. *Asia Commun. Photon. Conf. (ACP)* **AF2A.96** (2016).
28. Lu, H. H., Tsai, W. S., Huang, X. H., Jin, J. L., Xu, Y. Z., Chen, W. X., Lin, C. H. & Wu, T. M. Transmission of sub-terahertz signals over a fiber-FSO-5G NR hybrid system with an aggregate net bit rate of 227.912 Gb/s. *Opt. Express* **31**, 33320–33332 (2023).
29. Jia, S. et al. 0.4 THz photonic-wireless link with 106 Gb/s single channel bitrate. *IEEE/OSA J. Light. Technol.* **36**, 610–615 (2018).
30. Shin, D. C., Kim, B. S., Jang, H., Kim, Y. J. & Kim S. W. Photonic comb-rooted synthesis of ultra-stable terahertz frequencies. *Nat. Commun.* **14**, Art. no. 790 (2023).
31. Lu, H. H. et al. Simultaneous transmission of 5G MMW and sub-THz signals through a fibre-FSO-5G NR converged system. *IEEE/OSA J. Light. Technol.* **40**, 2348–2356 (2022).
32. Alshaikhli, Z. S., Hekmat, W. A., Al-Hamdani, A. H. & Hashim H. T. The spherical aberration correction by using bending and lens splitting: a compression. *AIP Conf. Proc.* **2398**, Art. no. 020005 (2022).
33. Lu, H. H. et al. A LEAF-FSO-wireless integrated system using DFB LD with multiple side modes injection locking. *IEEE/OSA J. Light. Technol.* **42**, 3684–3694 (2024).
34. Wang, C. et al. Beyond 300-Gbps/λ photonics-aided THz-over-fiber transmission employing MIMO single-carrier frequency-domain equalizer. *Opt. Lett.* **48**(6), 1363–1366 (2023).

Acknowledgements

This work was funded in part by the National Science and Technology Council of Taiwan (111-2221-E-027-031-MY3), in part by the Hsinchu Science Park Emerging Technology Application Program (112AO02B), and in part by the Qualcomm Technologies, Inc. (NAT-514839).

Author contributions

Ming-Chung Cheng, Hai-Han Lu, Hsiao-Mei Lin, Stotaw Talbachew Hayle, and Xu-Hong Huang contributed to the experiment design. Wei-Wen Hsu, Yu-Chen Chung, Yu-Yao Bai, Kelper Okram, and Jia-Ming Lu contributed to the experimental construction and measurement. Ming-Chung Cheng, Hai-Han Lu, Hsiao-Mei Lin, Stotaw Talbachew Hayle, and Xu-Hong Huang contributed to the data analysis. Ming-Chung Cheng, Hai-Han Lu, Hsiao-Mei Lin, and Stotaw Talbachew Hayle, contributed to the manuscript writing.

Funding

National Science and Technology Council, 111-2221-E-027-031-MY3, 111-2221-E-027-031-MY3,111-2221-E-027-031-MY3, 111-2221-E-027-031-MY3, 111-2221-E-027-031-MY3, 111-2221-E-027-031-MY3, 111-2221-E-027-031-MY3, Hsinchu Science Park Emerging Technology Application Program, 112AO02B, 112AO02B, 112AO02B, 112AO02B, 112AO02B, Qualcomm Technologies, Inc., NAT-514839, NAT-514839, NAT-514839, NAT-514839,NAT-514839.

Declarations

Competing interests

The authors declare no competing interests.

Additional information

Correspondence and requests for materials should be addressed to H.-H.L.

Reprints and permissions information is available at www.nature.com/reprints.

Publisher's note Springer Nature remains neutral with regard to jurisdictional claims in published maps and institutional affiliations.